High-energy 13.9 nm table-top soft-x-ray laser at 2.5 Hz repetition rate excited by a slab-pumped Ti:sapphire laser

D. H. Martz,[1,3] D. Alessi,[1] B. M. Luther,[1] Y. Wang,[1] D. Kemp,[1] M. Berrill,[1] and J. J. Rocca[1,2,4]

[1]National Science Foundation Engineering Research Center for Extreme Ultraviolet Science and Technology and Electrical and Computer Engineering Department, Colorado State University, Fort Collins, Colorado 80523, USA
[2]Physics Department, Colorado State University, Fort Collins, Colorado 80523, USA
[3] Dale.Martz@rams.colostate.edu
[4] rocca@engr.colostate.edu

Received February 23, 2010; revised April 12, 2010; accepted April 13, 2010; posted April 21, 2010 (Doc. ID 124604); published May 6, 2010

We have demonstrated repetitive operation of a table-top $\lambda = 13.9$ nm Ni-like Ag soft-x-ray laser that generates laser pulses with 10 μJ energy. The soft-x-ray laser is enabled by a Ti:sapphire laser pumped by high-repetition-rate frequency-doubled high-energy Nd:glass slab amplifiers. Soft-x-ray laser operation at 2.5 Hz repetition rate resulted in 20 microwatt average power. © 2010 Optical Society of America

OCIS codes: 140.7240, 340.7480, 140.3530.

There is significant interest in the table-top generation of high-average-power coherent soft-x-ray (SXR) radiation for applications. Powerful optical pump lasers have been used to generate picosecond duration SXR lasers in the 13 nm spectral region with energies of ~10–25 μJ at a rate of one shot every several minutes [1,2]. Recently high-repetition-rate table-top SXR lasers in this spectral range have reached energies up to ~1.5 μJ when pumped by 5–10 Hz repetition rate optical lasers [3–5]. These SXR lasers have been successfully used as the light source for table-top broad area microscopes with resolutions down to 38 nm [6,7]. This and other applications can significantly benefit from table-top SXR laser sources with higher average power.

In this Letter we report a significant increase in the pulse energy of multihertz table-top SXR lasers in the 13 nm spectral region utilizing a newly developed Ti:sapphire pump laser system driven by the frequency-doubled output of Nd:glass zig-zag slab amplifiers. Using this pump laser we have demonstrated $\lambda = 13.9$ nm laser pulses with maximum energies above 10 μJ. Operation of this SXR laser at 2.5 Hz repetition rate resulted in average power up to 20 μW and a 7% pulse energy fluctuation.

The SXR laser pulses were generated in a Ag plasma created and heated by a sequence of pulses from a chirped pulse amplification Ti:sapphire system comprising a mode-locked oscillator and three multipass amplifiers. The third amplification stage is pumped by up to 20 J of 527 nm light from the frequency-doubled output of a Nd:glass zig-zag slab laser developed in house. This dual-arm pump laser configuration (Fig. 1) was designed to operate at repetition rates of several hertz. It has long been recognized that the slab geometry has advantages that can overcome some of the limitations imposed by the more commonly used rod configuration [8,9]. The optical propagation along a zig-zag path, confined to the slab by total internal reflection, eliminates first-order thermal and stress-induced focusing. It also reduces stress-induced birefringence and allows for high-repetition-rate, high-average-power operation limited only by stress-induced fracture of the laser glass [10]. The slab geometry has been previously used to amplify nanosecond pulses to energies up to 25 J [11,12]. More recently, a picosecond chirped pulse amplification laser based on Nd:glass slab amplifiers has been used to pump SXR lasers at a repetition rate of 0.1 Hz, producing pulse energies up to ~1 μJ [13,14].

In our Ti:sapphire laser system, pulses from a Kerr lens mode-locked oscillator are stretched to 210 ps FWHM with a grating stretcher. The first two amplifier stages are pumped by a commercial 10 Hz frequency-doubled 800 mJ Q-switched Nd:YAG laser, resulting in 800 nm laser pulses with ~200 mJ energy, and the third multipass amplifier is pumped by the Nd:glass slab amplifiers. The front end of the slab laser consists of a Q-switched 1053 nm Nd:YLF oscillator that produces 1 mJ pulses of ~19 ns FWHM at a 5 Hz repetition rate. The pulses from the oscillator are directed through an active liquid crystal spatial light modulator (SLM) and are relay imaged onto a serrated aperture (SA) and then spatially filtered to

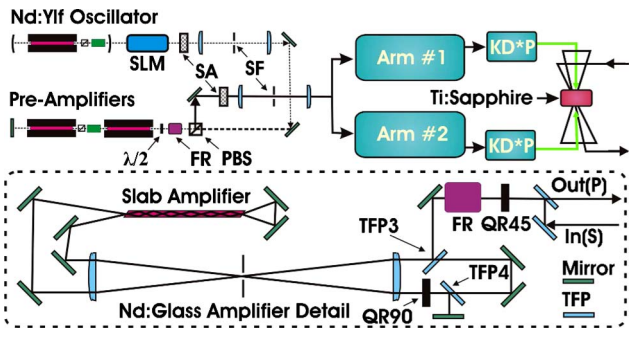

Fig. 1. (Color online) Top, block diagram of the third amplification stage of the Ti:sapphire pump laser system and associated slab amplifier laser system. Bottom, schematic diagram of the eight-pass Nd:glass slab amplifier.

produce a beam with a super-Gaussian intensity profile. The beam is then imaged into a preamplifier consisting of two 7 mm diameter Nd:YLF rods arranged in a double-pass configuration to yield pulse energies of ~120 mJ. The double pass is accomplished by using a polarizing beam splitter (PBS) cube, a Faraday rotator (FR) and a half-wave plate ($\lambda/2$) combination. The output of the preamplifier is imaged onto a second serrated aperture and spatial filter (SF) pair to obtain a flat-top beam profile. This profile is relay imaged throughout the rest of the system. The beam is subsequently stretched onto an oval of 8 mm $\times$ 120 mm dimension through a pair of cylindrical anamorphic imaging telescopes (not shown in Fig. 1) to conform to the 10 mm $\times$ 140 mm cross section of the slab amplifiers. The resulting beam is split into two identical arms by a 50% beam splitter, and each beam is amplified by eight passes through the 400 mm long slab amplifiers. The slabs are pumped by four Xe flashlamps, which are driven with a 300 μs electrical pulse, depositing ~700 J of electrical energy per lamp. Each arm operates in the following fashion. The input (S-polarized) beam reflects off a thin film polarizer (TFP) pair and travels through a 45° quartz rotator (QR45)/FR combination. The beam remains S polarized and is then injected into an eight-pass amplifier cavity by a third TFP (TFP3). With a relay imaging telescope, the pulses are directed into the slab for two passes of amplification. The same telescope images the beam back through a 90° quartz rotator (QR90), changing the polarization to P, resulting in transmission through TFP4. The beam is then reinjected along the path of the input beam (passing through TFP3) for an additional two passes through the slab. After a total of four passes the beam again passes through QR90, restoring the polarization to S, thereby causing it to be ejected by TFP4 to a normal incidence mirror. The mirror directs the beam back on itself, reversing the process for a total of eight passes before being sent back through the QR45/FR pair, resulting in P polarization and ejection by the input TFP.

Each slab amplifier arm generates pulses with an energy of up to 18 J that are frequency doubled in a pair of KD*P crystals to produce up to 10 J of $\lambda = 527$ nm light in each arm. Both beams are reshaped to 30 mm diameter and imaged into the 30-mm-thick third-stage Ti:sapphire amplifier rod. A near flat-top pump beam is achieved by adjusting the input beam's intensity profile by using the SLM. Three-pass amplification of the $\lambda = 800$ nm 200 mJ laser pulses through the third stage Ti:sapphire amplifier produces pulse energies up to 7.5 J at a 2.5 Hz repetition rate with a typical spatial profile shown in Fig. 2(b). Figure 2(a) shows a series of consecutive shots acquired while operating the amplifier at 1 Hz repetition rate. The shot-to-shot energy variation was measured to be ~1%.

The $\lambda = 13.9$ nm Ni-like Ag SXR laser was pumped, focusing 4.9 J of the total Ti:sapphire laser energy onto a ~30 μm FWHM wide, 6.3 mm FWHM long line on the surface of a polished 8 mm $\times$ 40 mm Ag slab target. The beam was split to create 210 ps prepulses with an energy of ~2.2 J that were directed at normal incidence onto the target to create a plasma with a large fraction of Ni-like Ag ions (Ag^{+19}). The remaining energy was directed into a vacuum grating compressor by using recently developed high-efficiency 800 nm dielectric gratings [15], producing 6 ps 2.7 J pulses. The plasma was allowed to expand to smooth the density gradient and was subsequently rapidly heated by the 6 ps pulse impinging at 23° grazing incidence. This inherently traveling wave pumping geometry takes advantage of the refraction of the pump beam in the electron density gradient of the precreated plasma to efficiently deposit energy into a plasma density region with optimum conditions for amplification [16,17]. The electron density in this region of the plasma is ~2.6×10^{20} cm^{-3}. The plasma is then rapidly heated to electron temperatures of up to ~550 eV, resulting in a transient population inversion that amplifies the $\lambda = 13.9$ nm $4d\ ^1S_0 \rightarrow 4p\ ^1P_1$ transition of Ni-like Ag into saturation. The highly monochromatic SXR laser output [Figs. 3(a) and 3(b)] was monitored by using the combination of a flat field spectrometer and a back-illuminated CCD detector. Five Zr filters with parylene support with a combined thickness of 2.3 μm were used to attenuate the SXR laser beam. The transmissivity of the combined set of filters was measured to be 1.4×10^{-4} by using a beamline of the ALS synchrotron at Berkeley.

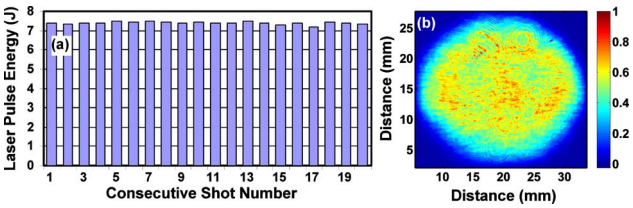

Fig. 2. (Color online) (a) Shot-to-shot variation of amplified $\lambda = 800$ nm Ti:sapphire laser pulse energy measured at a 1 Hz repetition rate. The average laser pulse energy is 7.4 J, and the standard deviation $\sigma = 1\%$. (b) Typical intensity profile of the amplified $\lambda = 800$ nm beam.

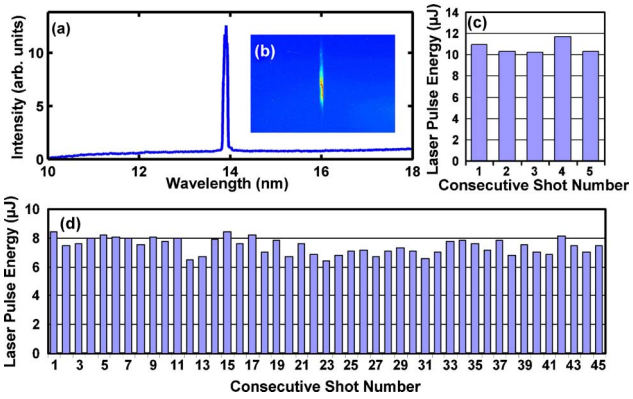

Fig. 3. (Color online) (a) Spectra of the Ni-like Ag plasma amplifier, showing highly monochromatic laser emission at $\lambda = 13.9$ nm. (b) Spectrally resolved CCD image of the laser output. (c) Laser output pulse energy of the $\lambda = 13.9$ nm laser operating at 0.5 Hz and (d) 2.5 Hz SXR laser operation with an average energy of 7.4 μJ with a shot-to-shot laser pulse energy variation of $\sigma = 7\%$.

SXR laser pulses with an energy exceeding 10 μJ were generated at 0.5 Hz repetition rate [Fig. 3(c)]. When the SXR laser was operated at a 2.5 Hz repetition rate, the average power reached 20 μW, the highest reported to date (to our knowledge) for a table-top SXR laser operating in the 13 nm spectral region. Figure 3(d) shows the shot-to-shot output pulse energy variation of the SXR laser operated at 2.5 Hz. The average pulse energy of this series of shots is 7.4 μJ with a standard deviation of 7%. This relatively good stability is the result of operating the SXR amplifier in a highly saturated regime. However, during day-to-day operation we measured average powers up to 20 μW with a standard deviation of 12%. The larger shot-to-shot variation with respect to that of the pump is likely to be due to the stability of the alignment of the prepulse and the short-pulse line focuses. The full angle beam divergence was measured to be 9.8 ± 0.5 mrad FWHM perpendicular to the target surface and 8.8 ± 0.5 mrad FWHM parallel to the target surface. The spatial coherence is expected to be similar to that reported in [18]. The SXR amplifier can be used to obtain pulses with full spatial and temporal coherence by employing the injection seeding technique demonstrated in [19]. The SXR laser pulse duration is expected to be similar to that which we previously measured for a transient 13.9 nm Ag laser excited at the same grazing incidence angle, ~5 ps [20]. Increasing the repetition rate to the design maximum of 5 Hz by compensating for second-order lensing effects in the slab laser can be expected to further increase the SXR laser average power. This table-top pump laser system was also used to create several microwatts of $\lambda = 13.2$ nm radiation from a Ni-like Cd SXR laser that permitted at-wavelength line-edge roughness measurements of patterned extreme ultraviolet lithography masks on a table top [21].

In conclusion, we have demonstrated a table-top $\lambda = 13.9$ nm SXR laser that produces pulse energies above 10 μJ. Operation at a 2.5 Hz repetition rate produced an average power of ~20 μW. High-repetition-rate operation of this laser is enabled by a newly developed Nd:glass zig-zag slab pump laser that is capable of pumping a high-energy Ti:sapphire amplifier at a repetition rate of several hertz with high shot-to-shot stability and good beam quality. This laser will make possible new applications of coherent SXR light requiring high average power on a table top.

This work was supported by the Engineering Research Centers Program of the National Science Foundation (NSF) under Award EEC-0310717.

References

1. J. Dunn, Y. Li, A. L. Osterheld, J. Nilsen, J. R. Hunter, and V. N. Shlyaptsev, Phys. Rev. Lett. **84**, 4834 (2000).
2. T. Kawachi, M. Kado, M. Tanaka, A. Sasaki, N. Hasegawa, A. V. Kilpio, S. Namba, K. Nagashima, P. Lu, K. Takahashi, H. Tang, R. Tai, M. Kishimoto, M. Koike, H. Daido, and Y. Kato, Phys. Rev. A **66**, 033815 (2002).
3. J. J. Rocca, Y. Wang, M. A. Larotonda, B. M. Luther, M. Berrill, and D. Alessi, Opt. Lett. **30**, 2581 (2005).
4. Y. Wang, M. A. Larotonda, B. M. Luther, D. Alessi, M. Berrill, V. N. Shlyaptsev, and J. J. Rocca, Phys. Rev. A **72**, 053807 (2005).
5. H. T. Kim, I. W. Choi, N. Hafz, J. H. Sung, T. J. Yu, K. H. Hong, T. M. Jeong, Y. C. Noh, D. K. Ko, K. A. Janulewicz, J. Tümmler, P. V. Nickles, W. Sandner, and J. Lee, Phys. Rev. A **77**, 023807 (2008).
6. G. Vaschenko, C. Brewer, F. Brizuela, Y. Wang, M. A. Larotonda, B. M. Luther, M. C. Marconi, J. J. Rocca, C. S. Menoni, E. H. Anderson, W. Chao, B. D. Harteneck, J. A. Liddle, Y. Liu, and D. T. Attwood, Opt. Lett. **31**, 1214 (2006).
7. F. Brizuela, Y. Wang, C. A. Brewer, F. Pedaci, W. Chao, E. H. Anderson, Y. Liu, K. A. Goldberg, P. Naulleau, P. Wachulak, M. C. Marconi, D. T. Attwood, J. J. Rocca, and C. S. Menoni, Opt. Lett. **34**, 271 (2009).
8. W. S. Martin and J. P. Chernoch, U.S. Patent 3,633,126 (January 4, 1972).
9. J. Eggleston, T. Kane, K. Kuhn, J. Unternahrer, and R. Byer, IEEE J. Quantum Electron. **20**, 289 (1984).
10. T. Kane, J. Eggleston, and R. Byer, IEEE J. Quantum Electron. **21**, 1195 (1985).
11. C. B. Dane, L. E. Zapata, W. A. Neuman, M. A. Norton, and L. A. Hackel, IEEE J. Quantum Electron. **31**, 148 (1995).
12. M. J. Shoup, J. H. Kelly, and D. L. Smith, Appl. Opt. **36**, 5827 (1997).
13. Y. Ochi, N. Hasegawa, T. Kawachi, and K. Nagashima, Appl. Opt. **46**, 1500 (2007).
14. Y. Ochi, T. Kawachi, N. Hasegawa, M. Nishikino, T. Ohba, M. Tanaka, M. Kishimoto, T. Kaihori, K. Nagashima, and A. Sugiyama, Jpn. J. Appl. Phys. Part 1 **48**, 120212 (2009).
15. D. H. Martz, H. T. Nguyen, D. Patel, J. A. Britten, D. Alessi, E. Krous, Y. Wang, M. A. Larotonda, J. George, B. Knollenberg, B. M. Luther, J. J. Rocca, and C. S. Menoni, Opt. Express **17**, 23809 (2009).
16. R. Keenan, J. Dunn, P. K. Patel, D. F. Price, R. F. Smith, and V. N. Shlyaptsev, Phys. Rev. Lett. **94**, 103901 (2005).
17. B. M. Luther, Y. Wang, M. A. Larotonda, D. Alessi, M. Berrill, M. C. Marconi, J. J. Rocca, and V. N. Shlyaptsev, Opt. Lett. **30**, 165 (2005).
18. Y. Liu, Y. Wang, M. A. Larotonda, B. M. Luther, J. J. Rocca, and D. T. Attwood, Opt. Express **14**, 12872 (2006).
19. Y. Wang, E. Granados, F. Pedaci, D. Alessi, B. Luther, M. Berrill, and J. J. Rocca, Nat. Photonics **2**, 94 (2008).
20. M. A. Larotonda, Y. Wang, M. Berrill, B. M. Luther, J. J. Rocca, M. M. Shakya, S. Gilbertson, and Z. Chang, Opt. Lett. **31**, 3043 (2006).
21. C. Menoni, F. Brizuela, Y. Wang, D. Alessi, S. Carbajo, B. Luther, A. Sakdinawat, W. Chao, Y. Liu, E. Anderson, K. Goldberg, D. Attwood, M. Marconi, and J. Rocca, presented by International Symposium on Extreme Ultraviolet Lithography, Prague, Czech Republic, 2009.